

StereoSpike: Depth Learning with a Spiking Neural Network

Ulysse Rançon^{1,2}, Javier Cuadrado-Anibarro¹, Benoit R. Cottureau¹, Timothée Masquelier¹

¹ Centre de Recherche Cerveau et Cognition (CERCO), CNRS UMR 5549, Université Toulouse 3, Toulouse, France

² Laboratoire d'Intégration du Matériau au Système (IMS), UMR CNRS 5218, Université de Bordeaux, Talence, France
ulysses.rancon@gmail.com, {javier.cuadrado, benoit.cottureau, timothee.masquelier}@cnrs.fr

Abstract

Depth estimation is an important computer vision task, useful in particular for navigation in autonomous vehicles, or for object manipulation in robotics. Here we solved it using an end-to-end neuromorphic approach, combining two event-based cameras and a Spiking Neural Network (SNN) with a slightly modified U-Net-like encoder-decoder architecture, that we named *StereoSpike*. More specifically, we used the Multi Vehicle Stereo Event Camera Dataset (MVSEC). It provides a depth ground-truth, which was used to train StereoSpike in a supervised manner, using surrogate gradient descent. We propose a novel readout paradigm to obtain a dense analog prediction—the depth of each pixel—from the spikes of the decoder. We demonstrate that this architecture generalizes very well, even better than its non-spiking counterparts, leading to state-of-the-art test accuracy. To the best of our knowledge, it is the first time that such a large-scale regression problem is solved by a fully spiking network. Finally, we show that low firing rates (<10%) can be obtained via regularization, with a minimal cost in accuracy. This means that StereoSpike could be efficiently implemented on neuromorphic chips, opening the door for low power and real time embedded systems.

1 Introduction

Depth is an important feature of the surrounding space whose estimation finds its place in various tasks across many different fields. Potential applications can be as diverse as object manipulation in robotics or collision avoidance for autonomous vehicles during navigation. In humans, depth processing is extremely well developed and relies on monocular (e.g., occlusions, perspectives or motion parallax) and binocular (retinal disparities) visual cues (Cutting and Vish-ton 1995). This processing consumes very little energy as the visual system encodes retinal information under the form of action potential, or *spikes* and it is believed that the brain only requires about 20 Watts to function (Mink, Blumens-chine, and Adams 1981). Over the last years, it has motivated the development of numerous bio-inspired approaches based on neuromorphic sensors and spiking neural networks to process depth in embedded systems.

Dynamic Vision Sensors (DVS) have recently gathered the interest of scientists and industrial actors, thanks to a growing number of research paper explaining how to process their output (Gallego et al. 2020). Reasons for this

recent popularity are the very high dynamic range, excellent temporal resolution and unrivaled energy efficiency of these event cameras, hence making them especially suitable in automotive scenarios with strong energy and latency constraints. Similarly, as retinal ganglion cells in the animal retina, their pixels asynchronously emit an action potential (i.e., a *spike*, or *event*) whenever the change in log-luminance at this location since the last event, reaches a threshold.

Spiking Neural Networks (SNNs) are a good fit for DVSSs, as they can leverage the sparsity of their output event streams. Implemented on dedicated chips such as Intel Loihi (Davies et al. 2018), IBM TrueNorth (Akopyan et al. 2015) or Brainchip Akida (Vanarse et al. 2019), these models could become a new paradigm for ultra-low power computation in the coming years. In addition, SNNs maintain the same level of biological plausibility as silicon retinæ, making them new models of choice among computational neuroscientists. SNNs have recently attracted the deep learning community since the breakthrough of Surrogate Gradient (SG) learning (Neftci, Mostafa, and Zenke 2019) (Zenke et al. 2021), which enabled the training of networks with back-propagation despite the non-differentiable condition for spike emission. While SNNs generally remain less accurate than their analog counterpart (i.e., Analog Neural Networks or ANNs), the gap in accuracy is decreasing, even on challenging problems like ImageNet (Fang et al. 2021b).

In this context, we propose an ultra-low power spiking neural network for depth estimation, capable of dense depth predictions even at places without events and performing on par with the current state-of-the-art. Despite the dynamic nature of DVS data, we show that the task of depth estimation from such neuromorphic event streams can be treated as a non-temporal task; therefore, our model is purely stateless in the sense that we reset all neurons to a membrane potential of zero at each timesteps. This feature certainly does not take advantage of the temporal processing abilities of SNNs, but reveals itself to decrease even further the computational and energy footprint of our model.

In section 2, we introduce a few related works that inspired our approach. We explain our methodology in section 3, including the data pre-processing, network architecture, and training details. In section 4, we compare our method

with prior studies in terms on performances. We also show that StereoSpike surpasses equivalent analog Neural Networks (ANNs) with similar architectures, both in terms of performances and energy-efficiency.

2 Related Work

Deep learning approaches for depth estimation have had a long tradition on the timescale of modern deep learning techniques. Initial methods were based on luminance-field data from traditional frame-based cameras, either in mono- or binocular setups. The model in (Eigen and Fergus 2015) was the first successful multi-scale architecture designed for depth estimation from RGB images, and was consequently followed by advances based on similar approaches (Mayer et al. 2016) (Li and Snavely 2018) (Godard, Aodha, and Brostow 2017).

Consistently with the recent interest of the scientific community in event cameras, a few works have successfully tackled the problem with neuromorphic data. Historically, several groups have used bio-inspired approaches such as Spiking Neural Networks (SNNs), in a very hardware-oriented direction, but not in a “deep learning” setting. For instance, the authors of (Risi, Calabrese, and Indiveri 2021) implemented a spike-based algorithm on a FPGA to regress low-resolution depth maps on a small size dataset. Furthermore, (Haessig et al. 2019) proposed a SNN for processing depth from defocus (DFD); this work targeted neuromorphic chips that enabled depth recover at full resolution, but the reconstruction was not dense.

Following the latter, (Zhu et al. 2019) presented a neural network that jointly predicted camera pose and per-pixel disparity from stereo inputs. However, their reconstructed depth maps remained sparse as they restricted their analyses to pixels where events occurred. The work in (Tulyakov et al. 2019) addressed this problem and pushed even further the state-of-the-art on indoor scenarios thanks to 3D convolutions exploiting a specific event embedding. In (Hidalgo-Carrio, Gehrig, and Scaramuzza 2020), dense metric depth was recovered from only one camera, and showed very good performances with a recurrent, monocular encoder-decoder architecture on outdoor sequences.

Another inspiration for our work has been the task of large-scale optical flow regression from neuromorphic data, which is very similar to depth reconstruction because it is also based on a large-scale image regression task with the same dataset. Similarly, large-scale optical flow regression from neuromorphic data has been an active area of research over the past few years, and has seen the emergence of methods with growing hardware-friendliness. EV-FlowNet (Zhu et al. 2018a), arguably considered as the precursor of encoder-decoder models for optical flow reconstruction from event data, consisted in a feedforward analog encoder-decoder architecture. As a direct sequel, the hybrid model Spike-FlowNet (Lee et al. 2020) made the effort of using spiking neurons in the encoder of a similar backbone, while maintaining the same levels of performances. On one hand, in this approach, spiking neurons were shown to be able of encoding abilities close to analog ones and at a reduced computational cost. On the other hand, authors kept the remain-

ing part of their network analog, to counteract the lack of expressivity in SNNs. More recently, the model proposed in (Paredes-Valles, Hagenars, and de Croon 2021) showed very good performances but it cannot be considered as a fully spiking network because real-value intermediate predictions of the outputs were reinjected within the network and mixed with binary spike tensors. In addition, they up-sampled low-scale representations with the bilinear upsampling method, which breaks the binary spike constraint necessary for an implementation on neuromorphic hardware. Nevertheless, it is the first success in a large-scale regression task with a network that is spiking for its vast majority.

So far, SNNs have been used for classification tasks like image recognition (Fang et al. 2021b), object detection (Perot et al. 2020), or motion segmentation (Parameshwara et al. 2021). Only a few works employed them for regression tasks. A notable exception is (Gehrig et al. 2020), but they only regressed 3 variables, while we propose here to regress the values of $260 \times 346 = 89960$ pixels.

3 Method

We used PyTorch and SpikingJelly¹ (Fang et al. 2020) as our main development libraries. PyTorch is currently one of the most popular tools for deep learning and automatic differentiation, while Spikingjelly is an open-source framework for spiking neural networks, based on PyTorch and with rising popularity. Our codes will be released on GitHub upon publication of the paper at the following address: <https://github.com/urancon/StereoSpike>

3.1 Dataset

We trained and tested our network on the Multi Vehicle Stereo Event Camera (MVSEC) dataset (Zhu et al. 2018b). Because of its large size and variability, it has become one of the most popular benchmarks for depth reconstruction from neuromorphic events. It was collected from two DAVIS346 cameras with a resolution of 346×260 pixels, mounted on several vehicles such as a car, a motorbike or a drone. The depth groundtruth was provided by a Velodyne Puck Lite LIDAR mounted on the top of the two event cameras and with a sampling frequency of 20 Hz, hence providing a depth map every 50 ms.

We applied our method on the *indoor flying* sequences of MVSEC, which was recorded on a quadricopter flying inside a large room. We used the data splits that were defined in (Zhu, Chen, and Daniilidis 2018) and (Tulyakov et al. 2019). We followed these previous works and removed take-off and landing parts of the sequence, because they contained very noisy event streams and inaccurate groundtruths.

3.2 Event Representation

We adopted a rather common representation of data: we binned all incoming spikes on each pixel on a time window of a given length, typically 50 ms. Furthermore, we accumulated spikes for each polarity in a different channels. Because there are two polarities, the input tensor had

¹<https://github.com/fangwei123456/spikingjelly>

a shape of $(2, Height, Width)$ and contained positive integers, corresponding to the number of spikes of each polarity that showed up at each position of the scene during the time window. We further refer to this format as *spike histograms* or *spike frames* interchangeably.

Many ANN approaches normalize this kind of input tensor (e.g. divide by the maximum number of spike count) for an easier-to-learn distribution of data and better generalization. We believe that this operation is not adapted to neuromorphic hardware, and can lead to non-integer number of spikes in the normalized input tensor. For this reason, we prefer feeding raw spike frames directly to our network.

Finally, we enhanced the input data with a temporal context by concatenating n subsequent frames channel-wise. As a result, the final input tensor has a shape of $(n \times 2, H, W)$.

3.3 Architecture

Our model was based on a U-Net backbone (Ronneberger, Fischer, and Brox 2015) consisting of an encoder, a bottleneck and a decoder whose non-linearities (activation functions) were replaced by spiking neurons. We used the Integrate-and-Fire (IF) model with a threshold potential of $v_{thresh} = 1.0$ and $v_{reset} = 0.0$.

Downsampling in the encoder was performed by 2-strided convolutions, which divided the spatial resolution by 2 while doubling the channel resolution. The bottleneck consisted in 2 SEWResBlocks (Fang et al. 2021a) following each other and with *ADD* connect function.

Because transposed convolutions are known to generate checkerboard artifacts (Odena, Dumoulin, and Olah 2016), we rather used nearest neighbor (NN) upsampling followed by a convolution. Contrarily to bilinear upsampling, we believe NN to be neuromorphic hardware friendly, because it essentially keeps integer spike counts in the upsampled volume. In terms of biological plausibility, it can be viewed as a single neuron at low scale projecting synapses towards several higher-scale neurons.

In addition, all layers in our network did not use a bias term nor Batch Normalization (BatchNorm) because adding constant biases is costly on neuromorphic hardware. Furthermore, they are not biologically plausible.

The output of the network was carried by the potentials of a pool of non-leaky neurons with an infinite threshold. Before each inference and like all neurons in the network, their membrane potentials were set to 0. One problem of SNNs is their lack of expressivity, since they can only update the membrane potentials of output neurons with discrete weighted spikes. With synapses coming from the full scale level of the encoder only, the model would always predict a “mean depth image” learned from the natural statistics of depth scenes: small depth values at the bottom and high values at the top of the prediction. To counteract this effect, we increased the number of spikes generated by lower levels (i.e. lower scales) of the network. Essentially, depth prediction layers consisted in nearest neighbor upsampling followed by convolution; they were the same as the upsampling layers in the decoder, except that they upsampled spike tensors directly up to the full, original scale.

3.4 Loss Function

Similarly as in (Hidalgo-Carrio, Gehrig, and Scaramuzza 2020), we used a combination of a multiscale regression loss with a multiscale regularization loss. Noting $R = \hat{D} - D$ the residual between the groundtruth depth map and intermediary i , the first term can be written as:

$$L_{regression} = \frac{1}{n} \sum_i (\sum_u (R(u))^2) - \frac{1}{n^2} (\sum_u R(u))^2 \quad (1)$$

where n is the number of valid groundtruth pixels u . With the same notations, the regularization loss is computed with:

$$L_{smooth} = \frac{1}{n} \sum_i \sum_u (|\nabla_x R_s(u)| + |\nabla_y R_s(u)|) \quad (2)$$

According to (Hidalgo-Carrio, Gehrig, and Scaramuzza 2020), the minimization of this term encourages smooth depth changes as well as sharp depth discontinuities in the depth map prediction, hence helping the network to represent objects that stand out of the background of the scene (e.g., because they are closer), while respecting its overall topology. Finally, we weighted both terms with a factor λ in the total loss:

$$L_{tot} = L_{regression} + \lambda L_{smooth} \quad (3)$$

We used a value of 0.5 for λ , which was determined empirically.

3.5 Training Procedure

Learning of parameter values in our model was done using surrogate gradient learning (Neftci, Mostafa, and Zenke 2019), as implemented in Spikingjelly Python library (Fang et al. 2020). We used arctan surrogate function for all IF spiking neurons.

Because our network is feed-forward and only processes one step for inference, we trained it with regular back-propagation, not Back-Propagation Through Time (BPTT) and on the shuffled dataset. We adopted the following procedure: 1) initialize all potentials (including output) to zero, 2) forward pass a sample or a batch of them, 3) calculate loss and back-propagate it, 4) update the weights and 5) start again with a new sample.

As explained in subsection 3.2, the input tensor consisted in $n = 5$ frames of 50 ms concatenated along channel dimension.

We used Adam optimizer (Kingma and Ba 2015) with $\beta_1 = 0.9$ and $\beta_2 = 0.999$. We trained the network for 30 epochs with an initial learning rate set to 2.10^{-4} and divided by 10 at epoch 8. Batch size was set to 1 and we did not use any weight decay.

4 Experiments

4.1 Performances

Our model performances are almost as good as those obtained from DDES (Tulyakov et al. 2019) (the current state

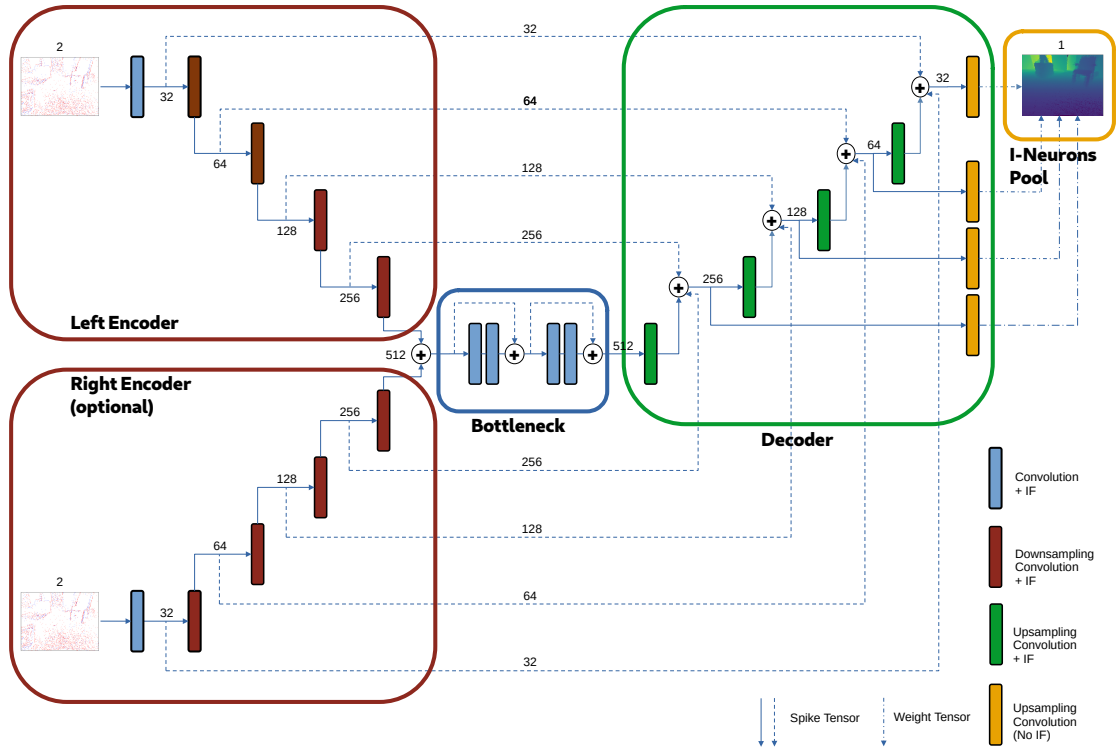


Figure 1: Detailed architecture of StereoSpike. Its encoder contains one or two branches (depending on the modality), each for a different DVS camera. The output of both branches are combined with a sum function, and further processed through a bottleneck consisting of 2 chained SEW-Resblocks. As a result, the tensor out of these residual layers is composed of integers in range $[0, 4]$. This latent representation is progressively upsampled by decoder layers and whose outputs are summed with same-level encoder spike tensors, leading to integer values in range $[0, 3]$. In parallel, prediction synapses from different scales directly project to output I-neurons whose potentials bear the final prediction. The numbers indicate the size of channel dimension for each spike volume. Best viewed in color.

of the art), which is a fully-fledged ANN using 3D convolutions within a less general framework. In addition, StereoSpike’s architecture is not specific to the estimation of depth and could be used for any other large-scale regression task. StereoSpike also performs better than TSES and CopNet, which by the way only predict depth at places where there have been events. Please refer to Figure 2 for qualitative visualizations of depth reconstructions obtained with our model and to Table 1 for a quantitative comparison with previous works on the Mean Depth Error (MDE), the most common metric used for characterizing depth estimation on the MVSEC.

In terms of MDE, performances obtained from the monocular and binocular encoders are similar. This suggests that in addition to being –for the most part– a non-temporal task, depth reconstruction from DVS data can be efficiently tackled on a monocular setting. The predictions of our model are mainly driven by monocular cues, but further work on the architecture could leverage the presence of a second event camera.

Table 1: Evaluation Mean Depth Error (MDE) in centimeters on several dataset splits of *indoor_flying* sequence. * indicates that the evaluation is done on the sparse groundtruth, i.e., only at pixels where events occurred

Model	MDE [cm]		
	Split 1	Split 2	Split 3
Tulyakov et al. (2019)	16.7	29.4	27.8
Ours (Binocular)	19.8	29.9	26.1
Ours (Monocular)	20.4	30.0	25.0
TSES*	36	44	36
CopNet*	61	100	64

4.2 StereoSpike - ANN comparison

A lesson learnt from our study and (Lee et al. 2020) is that SNNs can encode information very optimally, even with binary values. While Spike-FlowNet used ANNs to decode the latent space representation, we only use spiking neurons without mixing real-valued intermediary predictions with integer spikes as in (Paredes-Valles, Hagenaaars, and

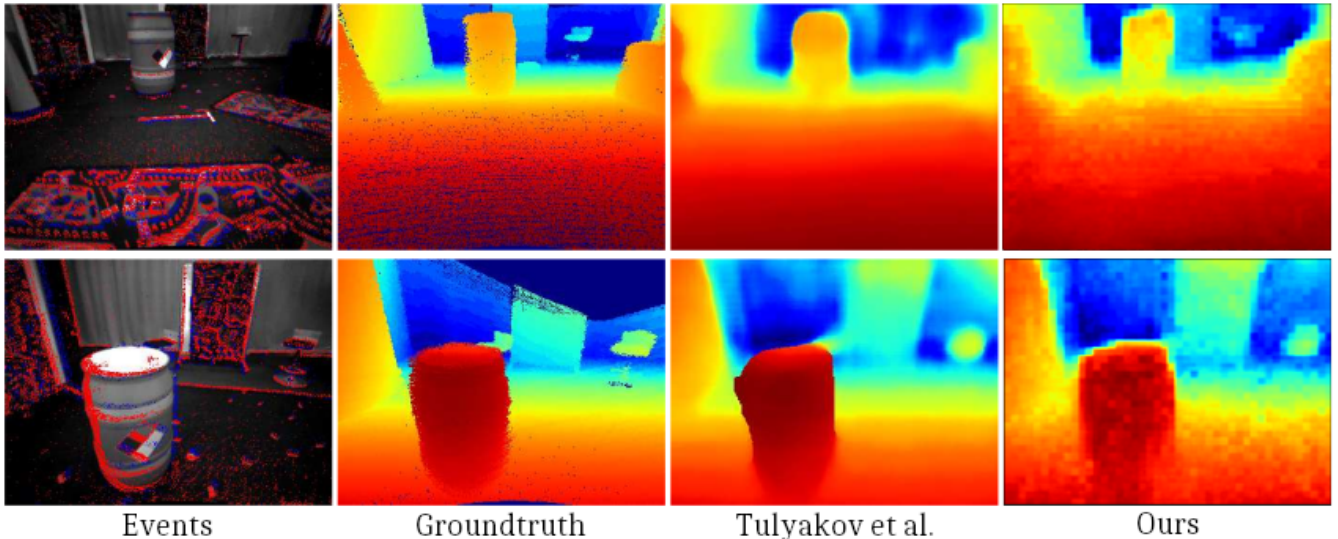


Figure 2: Qualitative comparison of our method with the current state-of-the-art detained by (Tulyakov et al. 2019). Similarly to what they did in their paper, we selected the same input frames and run our model to infer depth from this data; Event groundtruth and other prediction images were borrowed from their article. The top row corresponds to frame #1700 of *indoor_flying3* and frame #980 of *indoor_flying1* sequences. The pixelated aspect of our predictions comes from the Nearest-Neighbor interpolation in the prediction layer from very-low to full scale. Even so, it can be seen that our fully spiking network captures the scene just as well as a cutting edge ANN using a heavy framework and 3D convolutions. Adapted from (Tulyakov et al. 2019).

de Croon 2021). SNNs can therefore efficiently encode information as well as decode it, even for large scale regression tasks.

In an attempt to compare our model with fully-fledged ANNs, we trained equivalent ANN models. These models had a very similar architecture and output paradigm consisting in a pool of I-neurons; however, and with the idea of using the full power of analog models, we replaced IFN-odes by common activation functions, used Batch Normalization (BN) (Ioffe and Szegedy 2015) and trainable biases in convolution layers. Very surprisingly, these analog models showed much worse test metrics than their spiking counterparts (see Table 2). It suggests that SNNs have better generalization abilities than ANNs. To our knowledge, this is one of the few –if not the first– case of SNNs outperforming equivalent ANNs.

The LeakyReLU ANN achieves the lowest training loss and among the lowest training MDE, but has the worst test metrics by a large margin, hinting at a strong overfitting. Network with step-like activations (Sigmoid, Tanh) show better results on test sets and higher error on training sets, therefore suggesting a reduced overfitting phenomenon. Finally, the StereoSpike network –equivalent to an ANN with Heaviside step function as activation– achieves the best test loss and MDE but also the worst training metrics, therefore generalizing best, despite the absence of BN.

4.3 Computational Efficiency

In order to quantify the computational efficiency of our network, we report in table 3 the firing rates of its layers, i.e., the

Table 2: Comparative evaluation of our SNN vs equivalent ANN models on split 1 of *indoor_flying* sequence. For a given model, the train MDE, train loss and test loss are all sampled from the epoch yielding the best test MDE. Surprisingly, our fully spiking network surpasses by a large margin all of its analog relatives.

Model	MDE [cm]		Loss [au]	
	train	test	train	test
StereoSpike	15.7	19.8	0.97	1.34
ANN (Tanh + BN)	14.0	28.0	0.86	1.83
ANN (Sigmoid + BN)	11.6	28.2	0.80	1.56
ANN (LeakyReLU + BN)	12.3	34.9	0.74	1.69

density of intermediary tensors computed during inference. Sparse volumes can be leveraged by dedicated hardware capable of sparse computation, hence diminishing inference time as well as energy consumption.

It appears that the firing rates of our best model grow as layers become closer to the output I-neuron pool. We suggest that in this large-scale regression task, a minimum number of pre-synaptic spikes preceding output neurons is necessary to faithfully render the visual scene. Similarly, a certain amount of spikes could be necessary to encode the information contained in the input histograms.

To encompass this trade-off and estimate these minimal firing rates, we apply a regularization loss term explained in (Pellegrini, Zimmer, and Masquelier 2021) and train a

new binocular model on split 1. This secondary loss, which we also call *quadratic spike penalization loss*, penalizes the mean of the squared spike tensor. Therefore, for a given layer containing K spiking units whose output at time-step n is $S_k[n] \in \{0 \dots 4\}$, it can be defined as:

$$\begin{aligned} L_{spikes} &= \frac{1}{2NK} \sum_n \sum_k S_k[n]^2 \\ &= \frac{1}{2K} \sum_k S_k[n]^2 \end{aligned} \quad (4)$$

Because the number of time-steps to do one prediction is $N = 1$, as our model is purely stateless/feedforward. We apply this loss on the tensor out of the bottleneck *out_rconv* and on *out_addX* tensors, which the resulting tensors of the skip connections that are used by predictions layers at different scales. Penalizing these tensors also indirectly affects the activity of encoder layers, as their output conditions the density of same-level decoder volumes because of the skip connections. Therefore, this regularization is less aggressive than penalizing all intermediary tensors and performances are less negatively affected.

We then evaluate the network trained with spike penalization on its test set and compare obtained firing rates with our unconstrained model (see table 3). The regularized model show a drastic decrease in activity, at a very reasonable accuracy loss (~ 2 cm MDE). With these results, we can imagine our model implemented efficiently on dedicated hardware.

Target Hardware Our model has resolutely been developed in the philosophy of spiking neural networks. As a result, it is essentially implementable on dedicated neuromorphic hardware, such as Intel Loihi (Davies et al. 2018), IBM TrueNorth (Akopyan et al. 2015) or Brainchip Akida². These chips can leverage the binarity and sparsity of spike tensors navigating through the network. In addition, we believe that our model being feedforward and requiring a reset on all of its neurons at each timestep is not a problem, because resetting membrane potentials is actually less costly than applying a leak. Therefore, statelessness can be seen as an advantage over recurrence in spiking models with similar performances. However, we are aware that current neuromorphic chips are initially designed for the implementation of stateful units, and acknowledge that we do not leverage this feature. Consequently, we believe that it rather fits to dedicated hardware for stateless models with sparse activations quantized on 1 bit. This ideal target hardware does not exist yet, but we emphasize that our class of model with binary activations and less constrained weights provides a good compromise between Spiking Neural Networks (SNNs) and Binary Neural Networks (BNNs).

²<https://brainchipinc.com/about/>

Table 3: Detailed firing rates across layers of our network. *out_bottom* and *out_conv* spike tensors are the output of the encoders layers (Left or Right). *_combined* and *_add* spike tensors are sums of tensors at the end of encoders or skip connections. To be noted is that prediction layers take *_add* tensors as inputs, and their synapses project to the final neuron pool.

Layer	Density (%)	
	No Penalization	Penalization
<i>out_bottomL</i>	20.1	6.9
<i>out_conv1L</i>	7.6	7.1
<i>out_conv2L</i>	2.9	1.9
<i>out_conv3L</i>	4.4	2.3
<i>out_conv4L</i>	5.4	2.3
Left Encoder Mean	8.1	4.1
<i>out_bottomR</i>	11.4	5.7
<i>out_conv1R</i>	3.8	2.1
<i>out_conv2R</i>	2.2	1.3
<i>out_conv3R</i>	1.2	1.5
<i>out_conv4R</i>	0.3	0.5
Right Encoder Mean	3.8	2.2
<i>out_combined</i>	5.6	2.7
<i>out_resconv</i>	18.8	6.8
Bottleneck Mean	12.2	4.8
<i>out_deconv4</i>	20.4	7.9
<i>out_add4</i>	24.9	11.5
<i>out_deconv3</i>	16.3	4.3
<i>out_add3</i>	20.7	7.5
<i>out_deconv2</i>	23.1	2.2
<i>out_add2</i>	32.7	11.4
<i>out_deconv1</i>	38.1	0.5
<i>out_add1</i>	62.5	12.1
Decoder Mean	29.9	7.2
Model MDE [cm]	19.8	22.1

Handling integer (non-binary spike counts) Because of the sum operations present in residual layers of our architecture and at skip connections, bottleneck and decoder tensors can contain integer (non-binary) numbers of spikes. We explain here why we do not consider it as a problem. On most digital neuromorphic chips, spikes are represented by multi-bit messages containing destination and/or source addressing, and a few bits for a graded-value payloads; this is the case for Loihi, see (Davies et al. 2021). In our case, the spike counts are included in $[0, 4]$ and thus require at most 3 bits to encode. For the chips that can only handle binary spikes, a spike count of N could be handled by N serial binary spike operations

5 Conclusion

We have proposed StereoSpike, the first fully spiking, deep neural network architecture for large scale regression task with sparse activity. The key is expressivity and we tackle this problem by increasing the number of spikes generated

by deeper layers, with a pool of perfect integrator neurons bearing the final prediction with their membrane potential. The same strategy could presumably be used for other dense regression problems with SNNs, for example optic flow prediction.

We have shown that depth estimation from DVS data can be brought back to a stateless, static, non-temporal task. As a result, hardware implementations of StereoSpike could consume substantially less than recurrent versions. However, we are aware that our model neither takes advantage of this implicit recurrence of SNNs to capture temporal dependencies, nor of the very high temporal resolution of DVSs; these two aspects deserve investigation for further improvement of our algorithm.

Finally, our experiments hint towards the fact that because of the constraint on their output (i.e. binarity) SNNs might generalize better than their ANN counterparts. Consequently, our work is yet another evidence that binary encoding in latent space can represent input data as efficiently as real-valued projections. This encourages more research in the field of SNNs and neuromorphic computing in general, or Binarized Neural Networks (BNNs).

References

- Akopyan, F.; Sawada, J.; Cassidy, A.; Alvarez-Icaza, R.; Arthur, J.; Merolla, P.; Imam, N.; Nakamura, Y.; Datta, P.; Nam, G.-J.; Taba, B.; Beakes, M.; Brezzo, B.; Kuang, J. B.; Manohar, R.; Risk, W. P.; Jackson, B.; and Modha, D. S. 2015. TrueNorth: Design and Tool Flow of a 65 mW 1 Million Neuron Programmable Neurosynaptic Chip. *IEEE Transactions on Computer-Aided Design of Integrated Circuits and Systems*, 34(10): 1537–1557.
- Cutting, J.; and Vishton, P. 1995. *Perceiving layout and knowing distances: The integration, relative potency, and contextual use of different information about depth*. Academic Press.
- Davies, M.; Srinivasa, N.; Lin, T.-H.; Chinya, G.; Lines, A.; Wild, A.; Wang, H.; and Mathiakutty, D. 2018. Loihi: A Neuromorphic Manycore Processor with On-Chip Learning. *IEEE Micro*, PP: 1–1.
- Davies, M.; Wild, A.; Orchard, G.; Sandamirskaya, Y.; Guerra, G. A. F.; Joshi, P.; Plank, P.; and Risbud, S. R. 2021. Advancing Neuromorphic Computing With Loihi: A Survey of Results and Outlook. *Proceedings of the IEEE*, X: 1–24.
- Eigen, D.; and Fergus, R. 2015. Predicting Depth, Surface Normals and Semantic Labels with a Common Multi-scale Convolutional Architecture. In *2015 IEEE International Conference on Computer Vision (ICCV)*, 2650–2658.
- Fang, W.; Chen, Y.; Ding, J.; Chen, D.; Yu, Z.; Zhou, H.; Tian, Y.; and other contributors. 2020. SpikingJelly. <https://github.com/fangwei123456/spikingjelly>. Accessed: 2021-08-01.
- Fang, W.; Yu, Z.; Chen, Y.; Huang, T.; Masquelier, T.; and Tian, Y. 2021a. Deep Residual Learning in Spiking Neural Networks. arXiv:2102.04159.
- Fang, W.; Yu, Z.; Chen, Y.; Masquelier, T.; Huang, T.; and Tian, Y. 2021b. Incorporating Learnable Membrane Time Constant to Enhance Learning of Spiking Neural Networks. In *IEEE/CVF ICCV*.
- Gallego, G.; Delbruck, T.; Orchard, G. M.; Bartolozzi, C.; Taba, B.; Censi, A.; Leutenegger, S.; Davison, A.; Conradt, J.; Daniilidis, K.; and Scaramuzza, D. 2020. Event-based Vision: A Survey. *IEEE Transactions on Pattern Analysis and Machine Intelligence*, 1–1.
- Gehrig, M.; Shrestha, S. B.; Mouritzen, D.; and Scaramuzza, D. 2020. Event-Based Angular Velocity Regression with Spiking Networks. In *2020 IEEE International Conference on Robotics and Automation (ICRA)*, 4195–4202.
- Godard, C.; Aodha, O. M.; and Brostow, G. J. 2017. Unsupervised Monocular Depth Estimation with Left-Right Consistency. In *2017 IEEE Conference on Computer Vision and Pattern Recognition (CVPR)*, 6602–6611.
- Haessig, G.; Berthelon, X.; Ieng, S.-H.; and Benosman, R. 2019. A Spiking Neural Network Model of Depth from Defocus for Event-based Neuromorphic Vision. *Scientific Reports*, 9: 3744.
- Hidalgo-Carrio, J.; Gehrig, D.; and Scaramuzza, D. 2020. Learning Monocular Dense Depth from Events. *IEEE International Conference on 3D Vision (3DV)*.
- Ioffe, S.; and Szegedy, C. 2015. Batch Normalization: Accelerating Deep Network Training by Reducing Internal Covariate Shift. *CoRR*, abs/1502.03167.
- Kingma, D. P.; and Ba, J. 2015. Adam: A Method for Stochastic Optimization. *CoRR*, abs/1412.6980.
- Lee, C.; Kosta, A.; Zhu, A. Z.; Chaney, K.; Daniilidis, K.; and Roy, K. 2020. Spike-FlowNet: Event-based Optical Flow Estimation with Energy-Efficient Hybrid Neural Networks. In *European Conference on Computer Vision*, 366–382. Springer.
- Li, Z.; and Snavely, N. 2018. MegaDepth: Learning Single-View Depth Prediction from Internet Photos. *2018 IEEE/CVF Conference on Computer Vision and Pattern Recognition*, 2041–2050.
- Mayer, N.; Ilg, E.; Häusser, P.; Fischer, P.; Cremers, D.; Dosovitskiy, A.; and Brox, T. 2016. A Large Dataset to Train Convolutional Networks for Disparity, Optical Flow, and Scene Flow Estimation. In *2016 IEEE Conference on Computer Vision and Pattern Recognition (CVPR)*, 4040–4048.
- Mink, J. W.; Blumenschine, R. J.; and Adams, D. B. 1981. Ratio of central nervous system to body metabolism in vertebrates: its constancy and functional basis. *The American journal of physiology*, 241(3): R203–R212.
- Neftci, E. O.; Mostafa, H.; and Zenke, F. 2019. Surrogate Gradient Learning in Spiking Neural Networks: Bringing the Power of Gradient-Based Optimization to Spiking Neural Networks. *IEEE Signal Processing Magazine*, 36(6): 51–63.
- Odena, A.; Dumoulin, V.; and Olah, C. 2016. Deconvolution and Checkerboard Artifacts. *Distill*.
- Parameshwara, C. M.; Li, S.; Fermüller, C.; Sanket, N. J.; Evanusa, M.; and Aloimonos, Y. 2021. SpikeMS: Deep Spiking Neural Network for Motion Segmentation. *CoRR*, abs/2105.06562.

Paredes-Valles, F.; Hagenaars, J.; and de Croon, G. 2021. Self-Supervised Learning of Event-Based Optical Flow with Spiking Neural Networks. arXiv:2106.01862.

Pellegrini, T.; Zimmer, R.; and Masquelier, T. 2021. Low-Activity Supervised Convolutional Spiking Neural Networks Applied to Speech Commands Recognition. In *2021 IEEE Spoken Language Technology Workshop (SLT)*, 97–103. IEEE. ISBN 978-1-7281-7066-4.

Perot, E.; de Tournemire, P.; Nitti, D.; Masci, J.; and Sironi, A. 2020. Learning to Detect Objects with a 1 Megapixel Event Camera. In Larochelle, H.; Ranzato, M.; Hadsell, R.; Balcan, M. F.; and Lin, H., eds., *Advances in Neural Information Processing Systems*, volume 33, 16639–16652. Curran Associates, Inc.

Risi, N.; Calabrese, E.; and Indiveri, G. 2021. Instantaneous Stereo Depth Estimation of Real-World Stimuli with a Neuromorphic Stereo-Vision Setup. In *2021 IEEE International Symposium on Circuits and Systems (ISCAS)*, 1–5.

Ronneberger, O.; Fischer, P.; and Brox, T. 2015. U-Net: Convolutional Networks for Biomedical Image Segmentation. *CoRR*, abs/1505.04597.

Tulyakov, S.; Fleuret, F.; Kiefel, M.; Gehler, P.; and Hirsch, M. 2019. Learning an event sequence embedding for event-based deep stereo. In *Proceedings of the IEEE International Conference on Computer Vision (ICCV)*.

Vanarse, A.; Osseiran, A.; Rassau, A.; and van der Made, P. 2019. A Hardware-Deployable Neuromorphic Solution for Encoding and Classification of Electronic Nose Data. *Sensors*, 19(22).

Zenke, F.; Bohté, S. M.; Clopath, C.; Comşa, I. M.; Göltz, J.; Maass, W.; Masquelier, T.; Naud, R.; Neftci, E. O.; Petrovici, M. A.; Scherr, F.; and Goodman, D. F. 2021. Visualizing a joint future of neuroscience and neuromorphic engineering. *Neuron*, 109(4): 571–575.

Zhu, A.; Yuan, L.; Chaney, K.; and Daniilidis, K. 2018a. EV-FlowNet: Self-Supervised Optical Flow Estimation for Event-based Cameras. In *Proceedings of Robotics: Science and Systems*. Pittsburgh, Pennsylvania.

Zhu, A. Z.; Chen, Y.; and Daniilidis, K. 2018. Realtime Time Synchronized Event-Based Stereo. In Ferrari, V.; Hebert, M.; Sminchisescu, C.; and Weiss, Y., eds., *Computer Vision – ECCV 2018*, 438–452. Cham: Springer International Publishing.

Zhu, A. Z.; Thakur, D.; Ozaslan, T.; Pfrommer, B.; Kumar, V.; and Daniilidis, K. 2018b. The Multivehicle Stereo Event Camera Dataset: An Event Camera Dataset for 3D Perception. *IEEE Robotics and Automation Letters*, 3(3): 2032–2039.

Zhu, A. Z.; Yuan, L.; Chaney, K.; and Daniilidis, K. 2019. Unsupervised Event-Based Learning of Optical Flow, Depth, and Egomotion. In *2019 IEEE/CVF Conference on Computer Vision and Pattern Recognition (CVPR)*, 989–997.

also go to Wei Fang for his wonderful SpikingJelly library, without which this work would not have been possible. This research was supported by a grant from the ‘Agence Nationale de la Recherche’ (ANR-16-CE37-0002-01, ANR JCJC 3D3M) awarded to Benoit Cottureau.

6 Acknowledgments

We would like to thank Amirreza Yousefzadeh for his help and expertise on digital neuromorphic hardware. Our thanks